

**Ferromagnetic Ordering in Alkali-Metal Iron Antimonides:  $\text{NaFe}_4\text{Sb}_{12}$  and  $\text{KFe}_4\text{Sb}_{12}$** A. Leithe-Jasper,\* W. Schnelle, H. Rosner, N. Senthilkumaran, A. Rabis, M. Baenitz, A. Gippius,† E. Morozova,†  
J. A. Mydosh,‡ and Y. Grin*Max-Planck-Institut für Chemische Physik fester Stoffe, Nöthnitzer Straße 40, 01187 Dresden, Germany*

(Received 13 April 2003; published 18 July 2003)

New alkali-metal compounds with the filled-skutterudite structure were synthesized and their chemical and physical properties investigated. X-ray diffraction, microprobe, and chemical analysis established the structure and the composition without defects on the cation site. Magnetization, ac susceptibility, specific heat, resistivity, and NMR or NQR demonstrated  $\text{NaFe}_4\text{Sb}_{12}$  to be ferromagnetic below approximately 85 K and to exhibit an additional magnetic anomaly around 40 K. Band structure calculations find a large density of states at the Fermi energy and a ferromagnetic ground state. Similar behavior was observed for  $\text{KFe}_4\text{Sb}_{12}$ .

DOI: 10.1103/PhysRevLett.91.037208

PACS numbers: 75.50.Bb, 71.20.Lp, 75.40.Cx, 76.60.-k

Presently, there exists an enormous resurgence of interest in the generic class of compounds known as “skutterudites” [1,2]. These materials derive from the archetypal mineral skutterudite ( $\text{CoAs}_3$ ) and can be synthesized with the general formula  $MT_4X_{12}$ , where  $M$  is a rare-earth or an alkaline-earth metal,  $T$  is a transition metal of the iron or cobalt group, and  $X$  is a pnictide (P, As, or Sb) [3]. Recently, a plethora of topical behaviors has been observed with various rare-earth elements ranging from metal-insulator transitions to magnetic and quadrupole orderings, unconventional superconductivity, heavy fermion/non-Fermi liquids, and fluctuating/mixed valency [4,5]. Here, combinations of these effects can be tuned to coexist and interact. Another reason for the popularity of this family is its possible use in thermoelectric applications due to the low electric resistivity and large thermal power and resistivity [6].

Despite these intense efforts a number of fundamental properties remain unknown, as, for example, the relationship and interplay between the rare-earth and the transition metal [7]. Interestingly, for  $T = \text{Fe}$  the binaries  $\text{FeX}_3$  seem not to be stable under equilibrium conditions [8] and only filled variants are stable. Nevertheless, attention is usually focused on and dominated by the specific rare-earth element whose  $f$  electrons generate the above mentioned behaviors and less notice is taken of the  $T$  species and its contribution to the skutterudite physics.

In order to circumvent this ambiguity and to explore novel classes of non-rare-earth skutterudites, we successfully synthesized alkali-metal compounds. Now the “cage filler” is a light mass, single  $s$ -electron metal that is not magnetic or superconducting and contributes only marginally to the density of states of the valence band. When combined with  $T = \text{Fe}$ , we observe the unexpected appearance of long-range ferromagnetic order with rather small ordered moments at  $T_C \approx 85$  K enmeshed in a spectrum of strong spin fluctuations. The low ratio of the ordered moment and  $T_C$  sets the new compounds clearly apart from the known rare-earth filled skutteru-

rites. In fact, it is the first observation of magnetic ordering at the  $T$  sublattice in skutterudites. In this Letter, we examine the basic structural properties of  $\text{NaFe}_4\text{Sb}_{12}$  and  $\text{KFe}_4\text{Sb}_{12}$  through x-ray diffraction (XRD), electron probe microanalysis (EPMA), and chemical analysis. The physical properties were determined through bulk thermodynamic and transport measurements and by using nuclear resonance methods ( $^{23}\text{Na}$  NMR and  $^{121,123}\text{Sb}$  NQR) as local probes. The experimental data are supported by results of full-potential band structure calculations using the local spin density approximation (LSDA).

Because of the high vapor pressure of the alkali metals polycrystalline samples of  $\text{NaFe}_4\text{Sb}_{12}$  and  $\text{KFe}_4\text{Sb}_{12}$  were prepared in a two step synthesis. First, the binary compounds  $\text{NaSb}$  and  $\text{KSb}$  were synthesized. Then, a stoichiometric mixture of powdered monoantimonides together with  $\text{FeSb}_2$  and  $\text{Sb}$  was reacted at 400 °C for one week. Since binary alkali-metal antimony compounds are very sensitive to air the preparation was carried out in an Ar-atmosphere glove box system (oxygen and water less than 1 ppm). The ternary compounds were obtained as dark grey powders. In contrast to the binaries, they are relatively stable against air and moisture.

Physical property measurements were performed on specimens cut from compacted samples which were prepared by spark plasma sintering (SPS) the powders at 200 °C. Sample densities of 80% of the theoretical value could be achieved. Metallographic and EPMA investigation of polished specimens revealed elementary antimony as the only impurity phase present (less than 0.5 vol %).

Powder XRD data gave cubic (space group  $Im\bar{3}$ ) lattice parameters  $a = 9.1767(5)$  Å for  $\text{NaFe}_4\text{Sb}_{12}$  and  $a = 9.1994(5)$  Å for  $\text{KFe}_4\text{Sb}_{12}$ , respectively. Chemical analysis together with EPMA confirmed the stoichiometric composition. No indications of a defect occupation of the cation position were found. Single crystal XRD analysis of  $\text{NaFe}_4\text{Sb}_{12}$  corroborated the full occupancy of the

Na *2a* position inside the distorted icosahedral cages in the antimony-iron framework in full accordance with a filled-skutterudite structure of the  $\text{LaFe}_4\text{P}_{12}$  type [3,9]. Iron atoms are located on an *8c* position, Sb on a *24g* site. Sodium shows a large thermal displacement parameter ( $U_{\text{Na}} \approx 5U_{\text{Fe}} \approx 4U_{\text{Sb}}$ ) suggesting a “rattling” motion or static displacement inside the cavity. Thermal expansion of  $\text{NaFe}_4\text{Sb}_2$  was studied by low temperature powder XRD in the range from 15 to 300 K. A volume expansion of  $\Delta V/V(15 \text{ K}) = 0.71\%$  was observed in this temperature range; however, no indications for structural transitions were detected [9].

The field cooling (fc) and zero field cooling (zfc) magnetization as well as isothermal magnetization curves were measured. The new alkali-metal compounds  $\text{NaFe}_4\text{Sb}_{12}$  (Fig. 1) and  $\text{KFe}_4\text{Sb}_{12}$  were found to order ferromagnetically at  $T_C \approx 85 \text{ K}$ . For a sample of  $\text{NaFe}_4\text{Sb}_{12}$  (SPS treated) the remanent moment at 1.8 K is  $0.28\mu_B$  per Fe atom (Fig. 1 inset). The magnetization increases smoothly to  $0.60\mu_B$  in an external field of 14 T (not shown). Similar magnetization values are found for noncompacted  $\text{NaFe}_4\text{Sb}_{12}$  and  $\text{KFe}_4\text{Sb}_{12}$  samples. In the paramagnetic range an effective magnetic moment per Fe atom of  $1.6\text{--}1.8\mu_B$  can be extracted by a fit with a Curie-Weiss law for the two alkali-metal as well as for the Ba and Ca compounds. The paramagnetic Weiss temperature  $\Theta$  is positive and nearly identical with  $T_C$  for the alkali compounds. For  $\text{BaFe}_4\text{Sb}_{12}$ , which we use as a reference compound, the ferromagnetic interactions are much weaker ( $\Theta \approx +10\text{--}25 \text{ K}$ ), while they are remarkably strong for  $\text{CaFe}_4\text{Sb}_{12}$  ( $\Theta \approx +45 \text{ K}$ ). No bulk magnetic ordering down to 2 K was detected for the Ca and Ba compounds; however, an upturn of the fc susceptibility for low external fields and a much smaller zfc signal may indicate precursor effects of ferromagnetic ordering below approximately 20 K. All these findings indicate that a

bulk ferromagnetic state exists only for the alkali-metal filled compounds.

For the Na and K compounds a sharp peak was observed at  $T_C = 85 \text{ K}$  in the real part ( $\chi'$ ) of the ac susceptibility (Fig. 2). Around 40 K a strongly frequency-dependent maximum emerged in the imaginary part ( $\chi''$ ). This indicates a glasslike dynamical change in the magnetic state at this temperature well below  $T_C$ .

The electrical resistivities  $\rho(T)$  (not shown) of the Na, K, Ba, and Ca compounds are nevertheless similar: the  $\rho(T)$  curves increase in an “S” shape up to roughly 150 K above which they increase linearly.  $\rho(300 \text{ K}) \approx 1500 \mu\Omega \text{ cm}$  and thus the materials can be classified as “bad” metals. For the Na and K compounds tiny peaks are visible in  $\rho(T)$  at  $T_C$ . Below 20 K we find  $\rho - \rho_0 = AT^2$  with  $A = 1.780 \times 10^{-9}$  (Na) and  $1.207 \times 10^{-9} \Omega \text{ m K}^{-2}$  (K).

Heat capacity measurements were performed on  $\text{NaFe}_4\text{Sb}_{12}$  and  $\text{BaFe}_4\text{Sb}_{12}$  for  $1.8 \text{ K} < T < 300 \text{ K}$  using a relaxation method. The results confirm the existence of bulk ferromagnetism with a  $T_C \approx 85 \text{ K}$  for  $\text{NaFe}_4\text{Sb}_{12}$ , whereas for  $\text{BaFe}_4\text{Sb}_{12}$  no signs of magnetic order are observed (see Fig. 3). As a first approach we use  $\text{BaFe}_4\text{Sb}_{12}$  to estimate the magnetic contribution to the specific heat  $c_m(T)$  of  $\text{NaFe}_4\text{Sb}_{12}$ . Besides the phase transition at 85 K,  $c_m(T)$  shows an additional anomalous contribution around 30 K (see Fig. 3 inset), which is probably magnetic in origin. Similar evidence comes from above mentioned ac-susceptibility ( $\chi''$ ) data.

Staying with zero field values [10], for  $\text{NaFe}_4\text{Sb}_{12}$ , the linear electronic coefficient  $\gamma$  obtained for  $T < 14 \text{ K}$  is large ( $145 \text{ mJ mol}^{-1} \text{ K}^{-2}$ ). This yields a value of 62 states  $\text{eV}^{-1} \text{ f.u.}^{-1}$  (f.u. = formula unit) for the total density of states at the Fermi level,  $N(E_F)$ . For  $\text{BaFe}_4\text{Sb}_{12}$  the value of  $115 \text{ mJ mol}^{-1} \text{ K}^{-2}$  corresponding to  $N(E_F) = 50 \text{ states eV}^{-1} \text{ f.u.}^{-1}$  is found. For both ferromagnetic compounds the ratio  $A/\gamma^2$

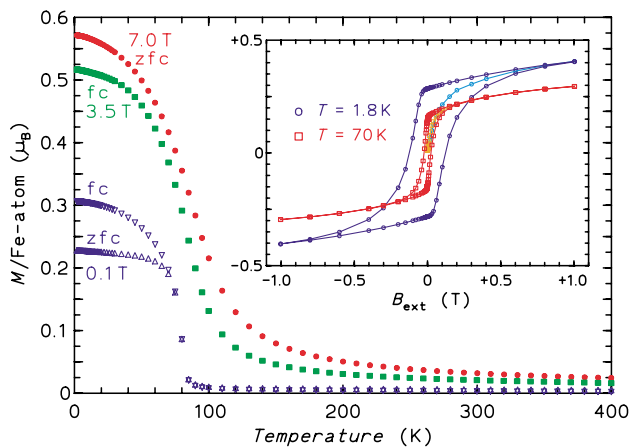


FIG. 1 (color online). Magnetization  $M(T)$  per Fe atom of  $\text{NaFe}_4\text{Sb}_{12}$ . The inset shows isothermal hysteresis loops at 1.8 and 70 K up to external fields of  $\pm 1 \text{ T}$ .

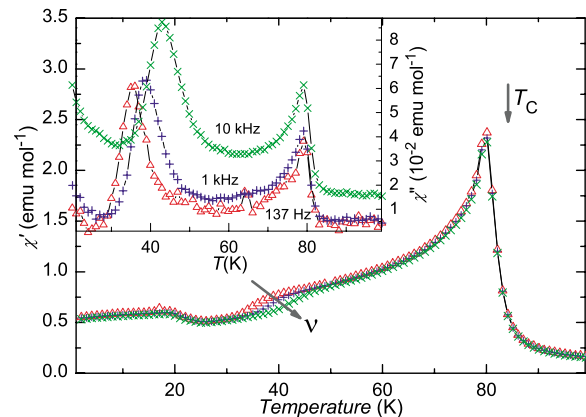


FIG. 2 (color online). Real part  $\chi'$  (main panel) and imaginary part  $\chi''$  (inset) of the ac magnetic susceptibility for  $\text{NaFe}_4\text{Sb}_{12}$  in a modulated field of 0.3 mT for different frequencies  $\nu$ .

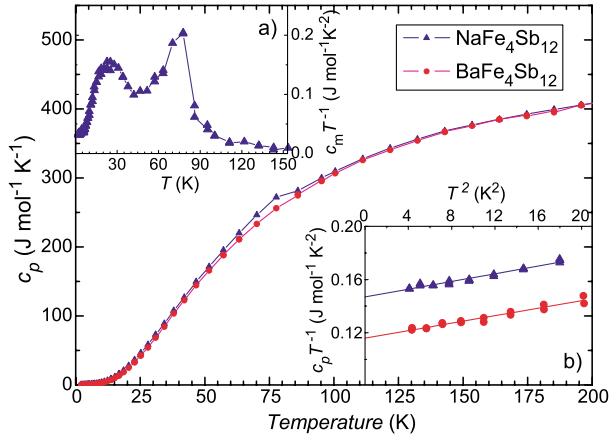


FIG. 3 (color online). Specific heat capacity of NaFe<sub>4</sub>Sb<sub>12</sub> and BaFe<sub>4</sub>Sb<sub>12</sub> vs temperature. (a) Magnetic contribution plotted as  $c_m/T$  vs  $T$ . (b)  $c_p/T$  vs  $T^2$  at low temperatures.

is near to the Kadowaki-Woods value of  $1.0 \times 10^{-7} \Omega \text{ m}(\text{mol K/J})^2$  [10].

NaFe<sub>4</sub>Sb<sub>12</sub> was investigated with <sup>23</sup>Na NMR spectroscopy ( $S = 3/2$ ;  $B_{\text{ext}} = 7.05$  T) in the temperature range from 4.2 to 290 K. The spin-lattice relaxation rate  $1/T_1$  was obtained by relaxation-recovery techniques. In agreement with structural investigations only one Na site was found at 290 K. The isotropic Knight shift  $K = -0.128(7)\%$  is negative in sign and points towards weak magnetic interaction at the sodium site. With decreasing temperature the system becomes more magnetic and the absolute value  $|K|$  becomes larger.  $|K(T)|$  shows the same overall behavior as the dc susceptibility. From the analysis of the  $K(\chi)$  plot (see Fig. 4), we could obtain two distinct hyperfine coupling constants  $A_\alpha$ :  $A_{\alpha 1} = -14.49 \text{ kOe}/\mu_B$  above  $T_C$  and  $A_{\alpha 2} = -11.55 \text{ kOe}/\mu_B$

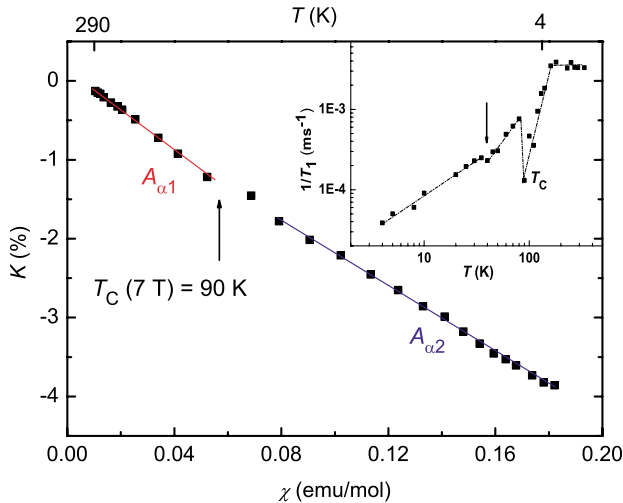


FIG. 4 (color online). Knight shift of <sup>23</sup>Na vs dc susceptibility  $\chi(T)$  with temperature as the implicit parameter for NaFe<sub>4</sub>Sb<sub>12</sub>. The inset shows inverse spin-lattice relaxation times  $1/T_1$  vs  $T$ .

below  $T_C$  in the ferromagnetic phase using the equation for a pure  $s$  orbital ( $A_\alpha = N_A \mu_B dK/d\chi_\alpha$ ). These relatively low values  $A_\alpha$  are in agreement with the small ordered magnetic moments of iron observed in both dc-magnetization experiments and local spin density approximation calculations (see below).

The plot of  $1/T_1(T)$  (Fig. 4 inset) shows linear dependence in the ferromagnetic region for  $T \rightarrow 0$ , thus obeying the Korringa relation [11] with a small anomaly between 30 and 40 K. The linear behavior is consistent with the results for  $|K|$  in the framework of Korringa theory, and  $c_p(T)$  and  $\chi_{\text{ac}}$  show similar features around 40 K. After a dip at  $T_C$   $1/T_1$  increases sharply in the paramagnetic state and becomes nearly constant around 160 K. This behavior is unusual, because for ferromagnets one expects a peak in  $1/T_1$  close to  $T_C$  usually attributed to strong spin fluctuations near  $T_C$  [11].

The antimony NQR spectrum (not shown) consists of five lines which are assigned to two transition lines for the <sup>121</sup>Sb ( $S = 5/2$ ) and three lines for <sup>123</sup>Sb ( $S = 7/2$ ). This assignment confirms the existence of only one crystallographic site according to the structure. Below  $T_C$  all lines decrease sharply to zero demonstrating the onset of the ferromagnetic ordering through an increase of the internal field at the antimony site.

A full-potential nonorthogonal local-orbital scheme [12] within the LSDA was used to obtain accurate electronic structure information. In the scalar relativistic calculations we used the exchange and correlation potential of Perdew and Wang [13]. Na ( $2s, 2p, 3s, 3p, 3d$ ), Fe ( $3s, 3p, 4s, 4p, 3d$ ), and Sb ( $4s, 4p, 4d, 5s, 5p, 5d$ ) states, respectively, were chosen as the basis set. All lower lying states were treated as core states. The Na  $3d$  states as well as the Sb  $5d$  states were taken into account to increase the completeness of the basis set. The inclusion of the Na ( $2s, 2p$ ), Fe ( $3s, 3p$ ), and Sb ( $4s, 4p, 4d$ ) states in the valence states was necessary to account for non-negligible core-core overlaps. The spatial extension of the basis orbitals, controlled by a confining potential [14]  $(r/r_0)^4$ , was optimized to minimize the total energy. A  $k$  mesh of 396 points in the irreducible part of the Brillouin zone was used.

The calculation results in a valence band of about 5 eV band width, formed mainly by Fe  $3d$  and Sb  $5p$  states (see Fig. 5). The density of states at the Fermi level is high with about 42 states  $\text{eV}^{-1} \text{ f.u.}^{-1}$ . In a spin polarized calculation, we find a ferromagnetic ground state with a total moment of  $2.97 \mu_B$  per cell. The main contribution comes from Fe ( $0.82 \mu_B$  per atom), while Sb ( $-0.02 \mu_B$ ) and Na ( $-0.05 \mu_B$ ) show slightly opposite spin polarization. Assigning magnetic moments to the Fe sites only, this results in  $0.74 \mu_B$  per Fe atom. The total energy of the ferromagnetic solution is lower by  $0.236 \text{ eV/f.u.}$  than that of the paramagnetic state.

To look for possible origins of magnetic anomalies, we have calculated the energy-versus-moment curve by fixed

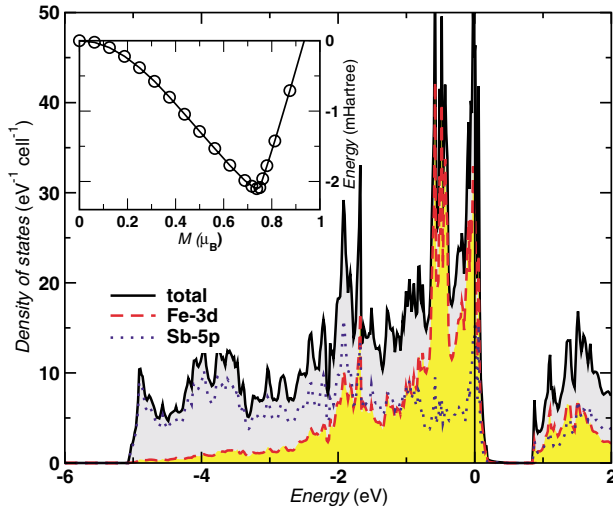


FIG. 5 (color online). Total, Fe-3d and Sb-5p derived density of states, respectively, for  $\text{NaFe}_4\text{Sb}_{12}$ . The contribution of Na to the valence band is negligible. The Fermi level is at zero energy. The inset shows the energy-versus-moment curve from fixed spin moment calculations.

spin moment calculations (see the inset in Fig. 5). We find a rather smooth curve with a clear minimum according to the unrestricted calculation mentioned above and no hint of other anomalies.

The size of the LSDA moment overestimates the experimental zero field moment of about  $0.3\mu_B$  considerably. A possible explanation could be the reduction of the ordered moment by strong spin fluctuations not included in the framework of LSDA. The basic theoretical difficulty in correcting LSDA results for this type of material is the separation of this nonincluded quantum-critical fluctuations from the dynamical fluctuations that are included [15]. A similar behavior is observed in  $\text{ZrZn}_2$ , in  $\text{Ni}_3\text{Al}$ , or in  $\text{FeAl}$ , where critical fluctuations reduce the moment strongly or even prevent magnetic ordering at all, respectively [15]. The increase of the magnetic moment in  $\text{NaFe}_4\text{Sb}_{12}$  to  $0.60\mu_B$  ( $0.65\mu_B$  extrapolating to  $1/H \rightarrow 0$ ) when suppressing critical fluctuations in a field of 14 T would be consistent with this explanation.

In conclusion, we have synthesized and fully characterized two new alkali-metal iron antimonides with the filled-skutterudite structure. Itinerant ferromagnetism below 85 K with a low saturation moment for both  $\text{NaFe}_4\text{Sb}_{12}$  and  $\text{KFe}_4\text{Sb}_{12}$  was established via a variety of thermodynamic and magnetic resonance measurements. These results are consistent with LSDA calculations. The small ratio of ordered moment and  $T_C$  as well as the site of the moments imply a completely different type of magnetic interactions compared to the rare-earth containing skutterudites. Experiments and calculations in order to determine the relationship between the appearance of ferromagnetism in the alkali compounds and the unique chemical bonding in filled-skutterudite structure

compounds are presently under way. Inspecting the electronic density of states already gives strong indication of significant hybridization of Fe 3d and Sb 5p states. As evidenced by a preliminary analysis of chemical bonding by electron localization function calculations [9], the Fe-Sb framework forms a unique rigid covalently bonded polyanion. Since the binary  $\text{FeSb}_3$  is metastable [8], the polyanion is stabilized by a charge transfer from the filler ion. The amount of charge transferred can be considered a coordinate on which the various electronic ground states of skutterudites occur. In addition, *d*-element spin fluctuations and *f* – *d* electron hybridization play an important role.

We are indebted to G. Auffermann, H. Borrmann, R. Cardoso-Gil, U. Burkhardt, and R. Ramlau for additional investigations and valuable discussions. A. R. acknowledges the Zeit-Stiftung for financial support.

\*Electronic address: jasper@cpfs.mpg.de

†Permanent address: Faculty of Physics, Moscow State University, Moscow, Russia.

‡Permanent address: Kamerlingh Onnes Laboratory, Leiden University, Leiden, The Netherlands.

- [1] See, for example, the collection of papers in the *Proceedings of the Strongly Correlated Electron System Conference, Krakow, 2002* [Acta Phys. Pol. B **34**, No. 2, 255–1638 (2003)].
- [2] C. Uher, *Semicond. Semimetals* **68**, 139 (2001).
- [3] W. Jeitschko and D. Braun, *Acta Crystallogr. Sect. B* **33**, 3401 (1977).
- [4] E. D. Bauer *et al.*, *Phys. Rev. B* **65**, 100506 (2002); E. Bauer *et al.*, *ibid.* **66**, 214421 (2002); A. Grytsiv *et al.*, *ibid.* **66**, 094411 (2002).
- [5] R. Vollmer *et al.*, *Phys. Rev. Lett.* **90**, 057001 (2003); H. Kotegawa *et al.*, *ibid.* **90**, 027001 (2003); R. Viennois *et al.*, *Acta Phys. Pol. B* **34**, 1221 (2003).
- [6] G. A. Slack and V. G. Tsoukala, *J. Appl. Phys.* **76**, 1665 (1994); B. C. Sales, D. Mandrus, B. C. Chakoumakos, V. Keppens, and J. R. Thompson, *Phys. Rev. B* **56**, 15081 (1997).
- [7] M. E. Danebrock, C. B. H. Evers, and W. Jeitschko, *J. Phys. Chem. Solids* **57**, 381 (1996).
- [8] M. D. Hornbostel, E. J. Hyer, J. H. Edvalson, and D. C. Johnston, *Inorg. Chem.* **36**, 4270 (1997).
- [9] A. Leithe-Jasper *et al.* (unpublished).
- [10] Spin fluctuations play a minor role at  $T \ll T_{SF} \approx T_C$ . See, e.g., K. Ikeda, S. K. Dhar, M. Yoshizawa, and K. A. Gschneidner, Jr., *J. Magn. Magn. Mater.* **100**, 292 (1991).
- [11] Y. Yamada and A. Sakata, *J. Phys. Soc. Jpn.* **54**, 4321 (1985); K. Yoshimura *et al.*, *ibid.* **56**, 1138 (1987).
- [12] K. Koepf and H. Eschrig, *Phys. Rev. B* **59**, 1743 (1999).
- [13] J. P. Perdew and Y. Wang, *Phys. Rev. B* **45**, 13244 (1992).
- [14] H. Eschrig, *Optimized LCAO Method and the Electronic Structure of Extended Systems* (Springer, Berlin, 1989).
- [15] P. Larson, I. I. Mazin, and D. J. Singh, *cond-mat/0305407*.